Crafting a Clearer Crystal Ball for ENSO

Andrew T. Wittenberg*, Fanrong J. Zeng, Thomas L. Delworth, William F. Cooke, and the GFDL-SPEAR Development Team

NOAA Geophysical Fluid Dynamics Laboratory, Princeton, New Jersey

1. Introduction and Models

The **El Niño/Southern Oscillation (ENSO)** impacts economies & ecosystems worldwide, and reliable outlooks for ENSO risks depend on realistic global models. **SPEAR** (***S**eamless System for **P**rediction and **EA**rth System **R**esearch*; Delworth et al. 2020) is a suite of global coupled GCMs recently developed by GFDL, using the same core configuration as the CM4 & ESM4 models (Held et al. 2019; Dunne et al. 2020) whose ENSO simulations rank among the best of the CMIP6 models (Planton et al. 2021; Chen et al. 2021). SPEAR is optimized for seasonal-to-centennial climate research, data assimilation, forecasts, & projections, contributing global seasonal forecasts each month as part of the North American Multi-Model Ensemble (NMME). **SPEAR_MED** has a 0.5° atmosphere/land grid, with a 1° ocean/ice grid (refined to Δy=0.33° near the equator). **SPEAR_MED_FA** further corrects the simulated climatological SST, SSS, & wind stress by adding "flux adjustments" (**FA**, **Fig. 1**) to the air→sea fluxes. Here we examine **5-member ensembles** from these models, run with **CMIP6 historical** (1921–2014) and **SSP5-8.5 projected** (2015–2100) forcings.

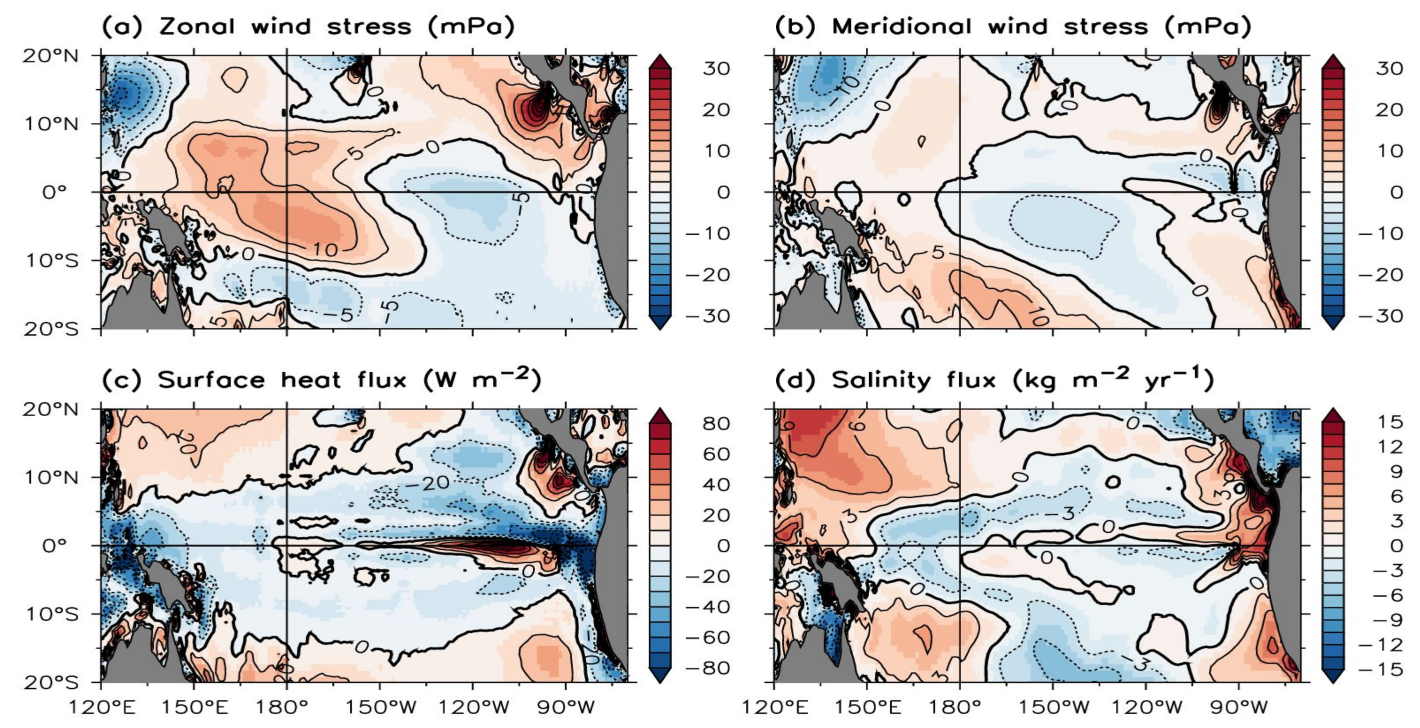

Fig. 1: Annual mean of the surface **flux adjustments** prescribed in SPEAR_MED_FA, here highlighting the tropical Pacific. The FA is seasonally-varying & interannually-repeating, and applied over the global oceans (90°S–65°N) for vector wind stress, and over the tropical oceans (30°S–30°N) for heat & salt.

2. Tropical Background Climate

SPEAR_MED simulates a realistic tropical climate (**Fig. 2**), though some biases are evident: the equatorial Pacific (eqPac) cold tongue is too cold & dry, the warm pool & the "double" ITCZ of the southeast tropical Pacific are too wet, and the equatorial thermocline is too shallow. FA mitigates these biases by heating the cold tongue & weakening the equatorial trade winds; yet the warm pool remains too wet, pointing to an intrinsic bias in the atmosphere component.

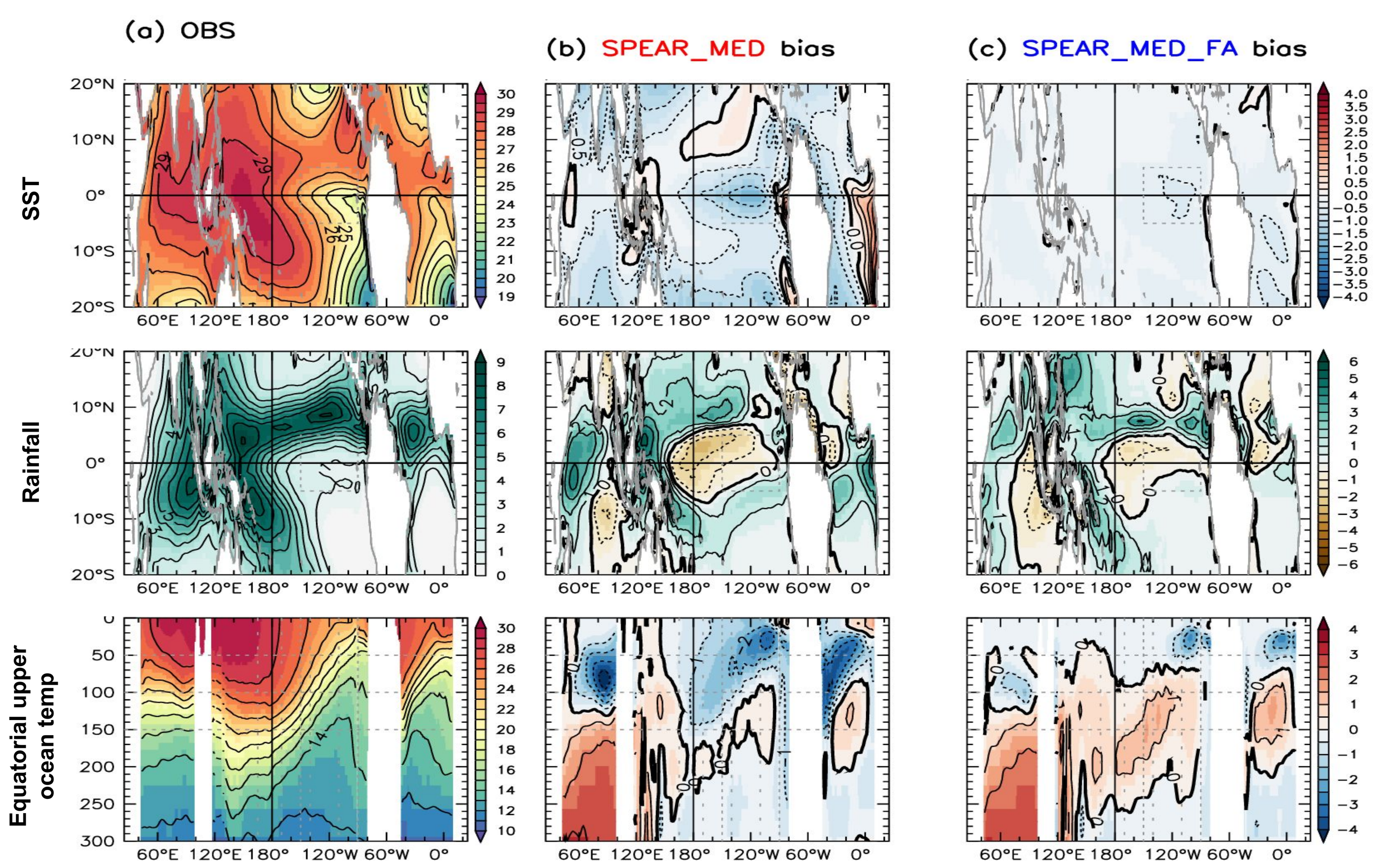

Fig. 2: Tropical 1979–2016 annual-mean climatological fields from (a) observational totals, (b) SPEAR_MED bias, and (c) SPEAR_MED_FA bias. Rows show **SST** (Row 1, °C; obs from OISST.v2), **rainfall** (Row 2, mm day^{-1}; obs from GPCP.v2.3), and **equatorial ocean temperature** (Row 3, °C; obs from ORA-S4). The model climatologies represent 5-member ensemble means.

4. ENSO Simulation Performance

SPEAR_MED simulates a realistic ENSO (**Figs. 3–7**), including the SST anomaly (SSTA) amplitude, period, spectrum, interdecadal modulation, seasonal synchronization, and remote teleconnections to the Pacific/North America (PNA) pattern; yet the model also underestimates the observed rain variance in the central equatorial Pacific. **FA improves the simulation** by: weakening the SSTA variance and strengthening the rain & wind responses in the west/central eqPac; intensifying the eqPac SSTA damping from cloud shading & evaporation; enhancing the positive skewness of eastern eqPac SSTs; strengthening the tendency of ENSO events to peak in Oct-Dec; lengthening ENSO's period; and broadening ENSO's spectral peak.

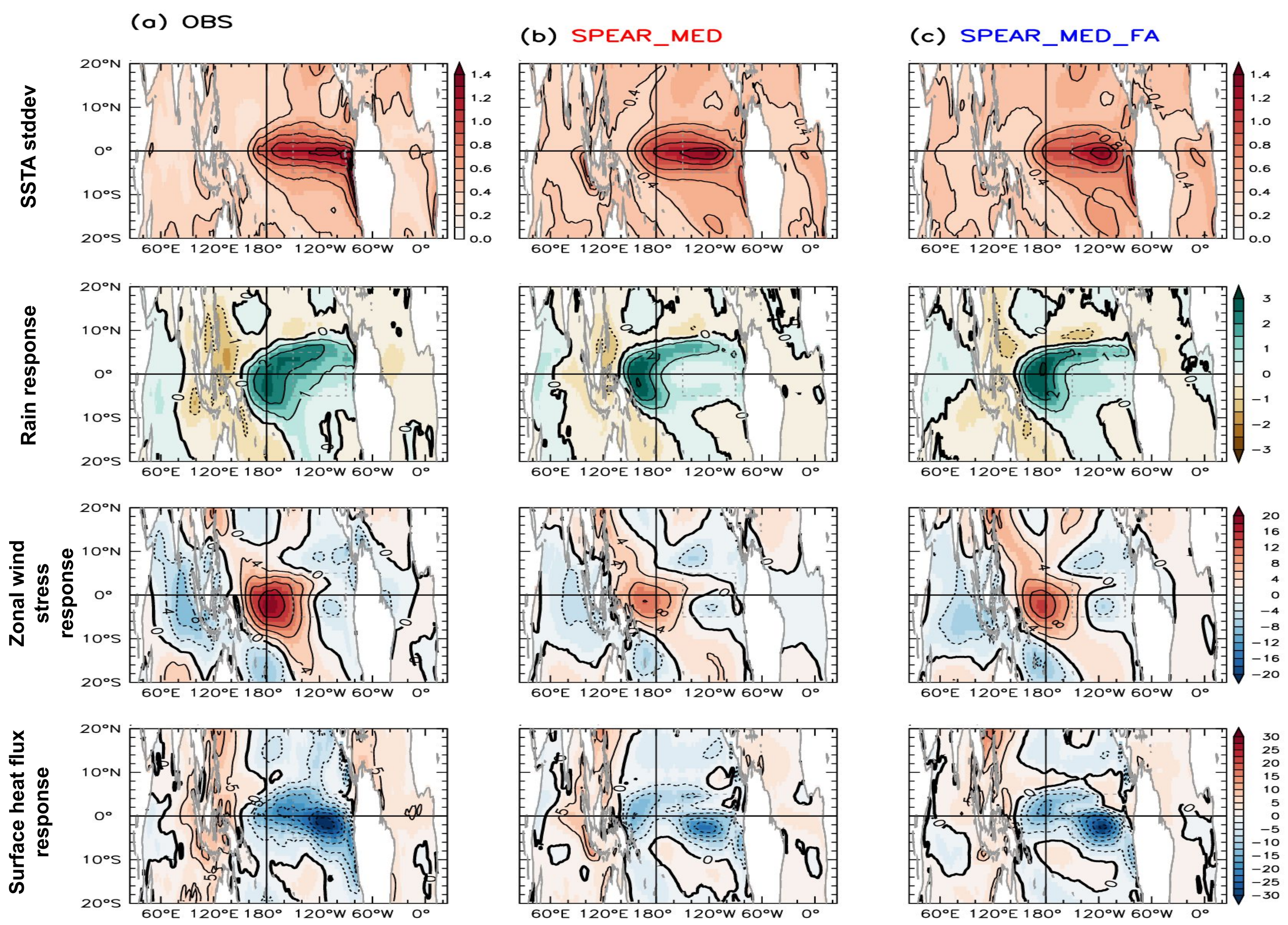

Fig. 3: Tropical 1979–2016 ENSO patterns from (a) observations, (b) SPEAR_MED, (c) SPEAR_MED_FA. Row 1 shows the stddev of 1 yr low-passed **SSTAs** (K; obs from OISST.v2). Remaining rows are monthly anomalies regressed onto NINO3 SSTAs (150°W–90°W, 5°S–5°N; dashed gray box), for **rainfall** (Row 2, mm day^{-1} K^{-1}; obs from GPCP.v2.3), **zonal wind stress** (Row 3, mPa K^{-1}; positive for eastward stress on the ocean; obs from ERA-Interim), and **net surface heat flux** (Row 4, W m^{-2} K^{-1}; positive for heating of the ocean; obs from ERA-Interim). Model fields represent 5-member ensemble means of the computed statistics.

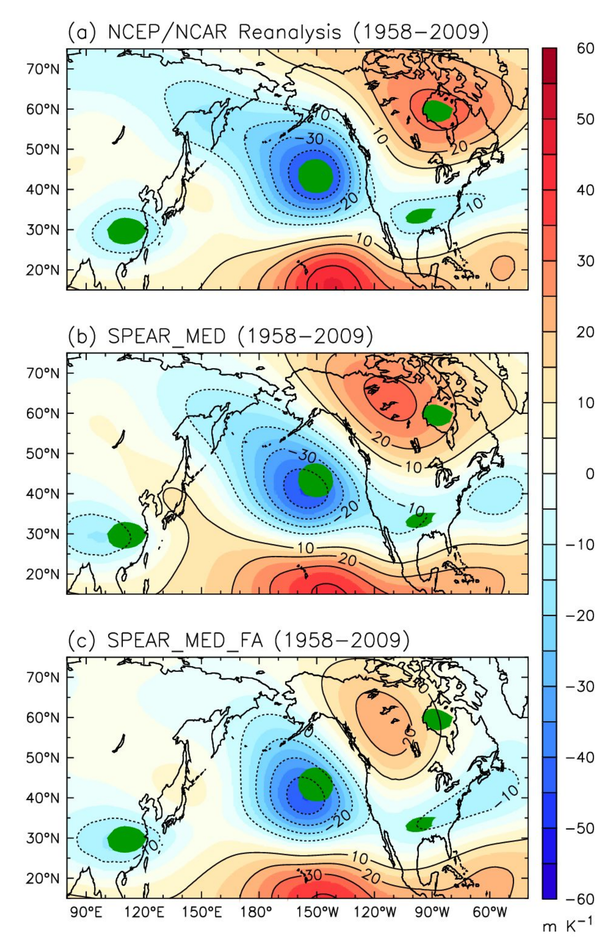

Fig. 4: **DJF 200 hPa geopotential height** anomalies regressed onto DJF NINO3 SSTAs (m K^{-1}) during 1958–2009, after detrending via a 20 yr high pass filter. (a) Obs from the NCEP/NCAR reanalysis. Also shown are 5-member ensemble-mean regressions from (b) SPEAR_MED and (c) SPEAR_MED_FA. Green spots are the observed extrema from (a).

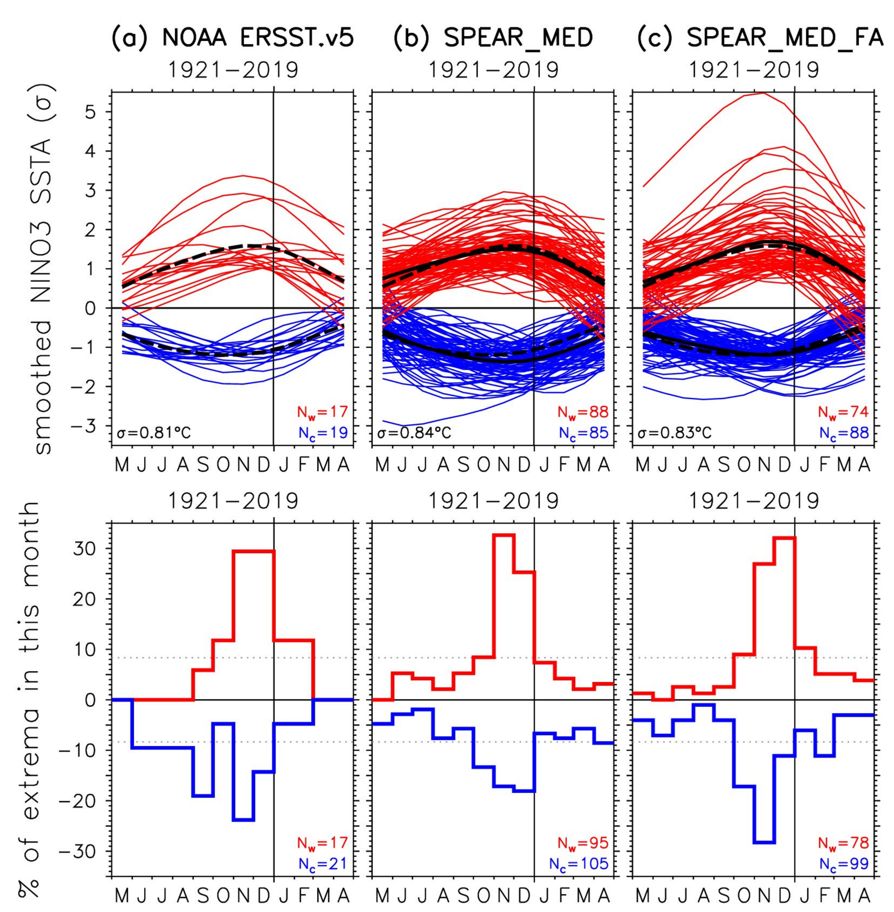

Fig. 5: Top row: evolution of 7-month triangle-smoothed **NINO3 SSTA** (units of stddev, σ) during May–April, for the N_w **warm events** and N_c **cold events** in the time series for which the smoothed NINO3 SSTA exceeds 1 K during 1921–2019. Events are extracted from (a) ERSST.v5 obs; and the 5 members of (b) SPEAR_MED and (c) SPEAR_MED_FA. Dashed black lines are the observed composite mean events from (a), and solid black lines are the simulated composites. Bottom row: histograms of **peak calendar months** for the warm & cold events in the top row.

5. ENSO Dynamics and Projected Future Changes

SPEAR_MED's cold/dry bias along the equator (**Fig. 2b**) inhibits its eastward & equatorward shifts of convection & rainfall during El Niño (**Fig. 3b**), which affects its ENSO behavior, feedbacks, and teleconnections (**Figs. 4–7**). The FA version corrects the seasonal cycle of SST & winds, enhancing the **seasonal links between the ITCZs and the eqPac** ocean waveguide, improving ENSO's seasonal timing. FA also strengthens the ENSO **cloud shading response**, damping the SSTAs in the west/central eqPac. The FA further strengthens & broadens the eqPac westerly wind anomalies during El Niño, boosting the **thermocline feedback** and slowing the **poleward discharge of upper ocean heat** from the eqPac, lengthening the ENSO period. FA does not improve the residual damping of eqPac SSTA by submonthly processes, which is weaker in SPEAR_MED than in the reanalysis; this may stem from the relatively coarse (1°) zonal grid of SPEAR_MED's ocean component, which cannot fully resolve the vigorous stirring & mixing associated with tropical instability waves (TIWs).

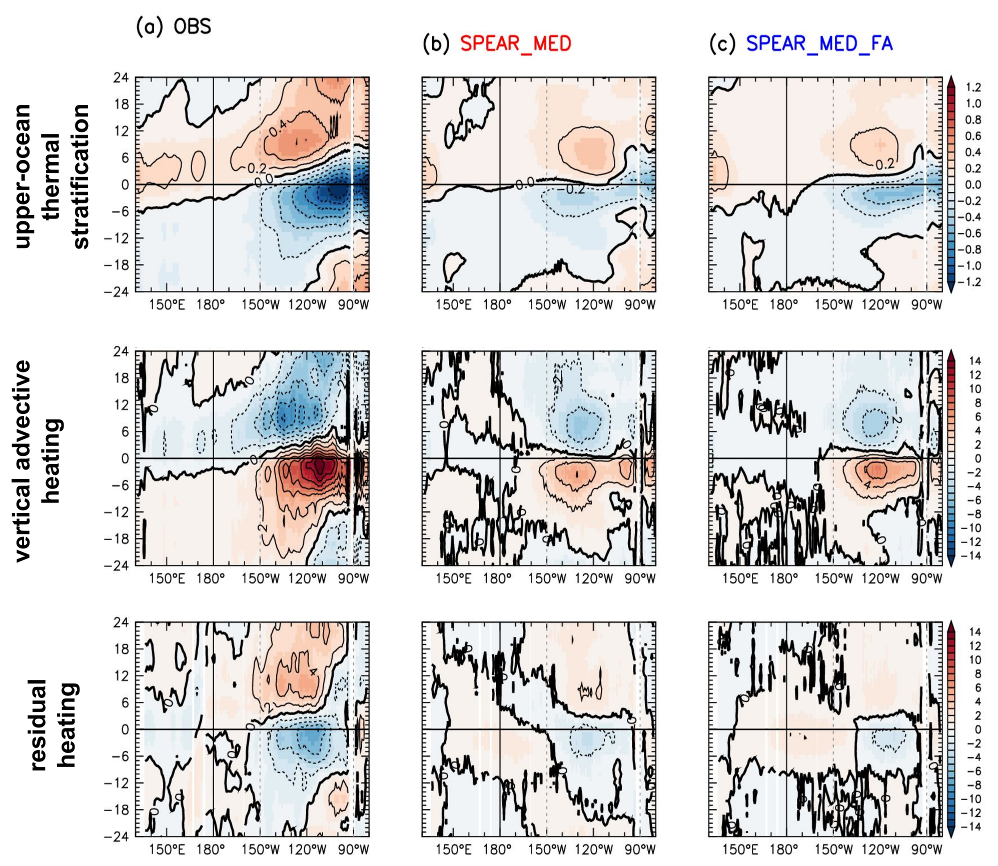

Fig. 6: Time vs. longitude plots of monthly equatorial Pacific **subsurface anomalies, regressed onto time-lagged NINO3 SSTA** during 1979–2014. Ordinate is the lag (in months) after the event's NINO3 SSTAs peak at lag 0; time evolves upward. Columns show (a) ORA-S4 obs, and 5-member ensemble-mean regressions from (b) SPEAR_MED and (c) SPEAR_MED_FA. Rows show regressions of anomalous **thermal stratification**, i.e. SST minus 50 m temperature (Row 1, K K^{-1}); anomalous **vertical advective heating** by monthly means, averaged over the top 50 m (Row 2, K yr^{-1} K^{-1}); and anomalous **residual heating** (due mainly to submonthly mixing & stirring), i.e. the total temperature tendency minus the heating from total monthly advection & air-sea heat fluxes, averaged over the top 50 m (Row 3, K yr^{-1} K^{-1}).

SPEAR_MED projects **stronger future ENSO anomalies** of SST & rainfall (**Fig. 7**). The FA version, whose historical rain variance agrees better with obs, projects an even **greater increase** in future NINO3.4 rain extremes, due in part to the reduced background SST contrast between the Pacific cold tongue & warm pool. While SPEAR_MED projects a robustly shorter period for ENSO in 2051–2100, this is less evident in the FA version.

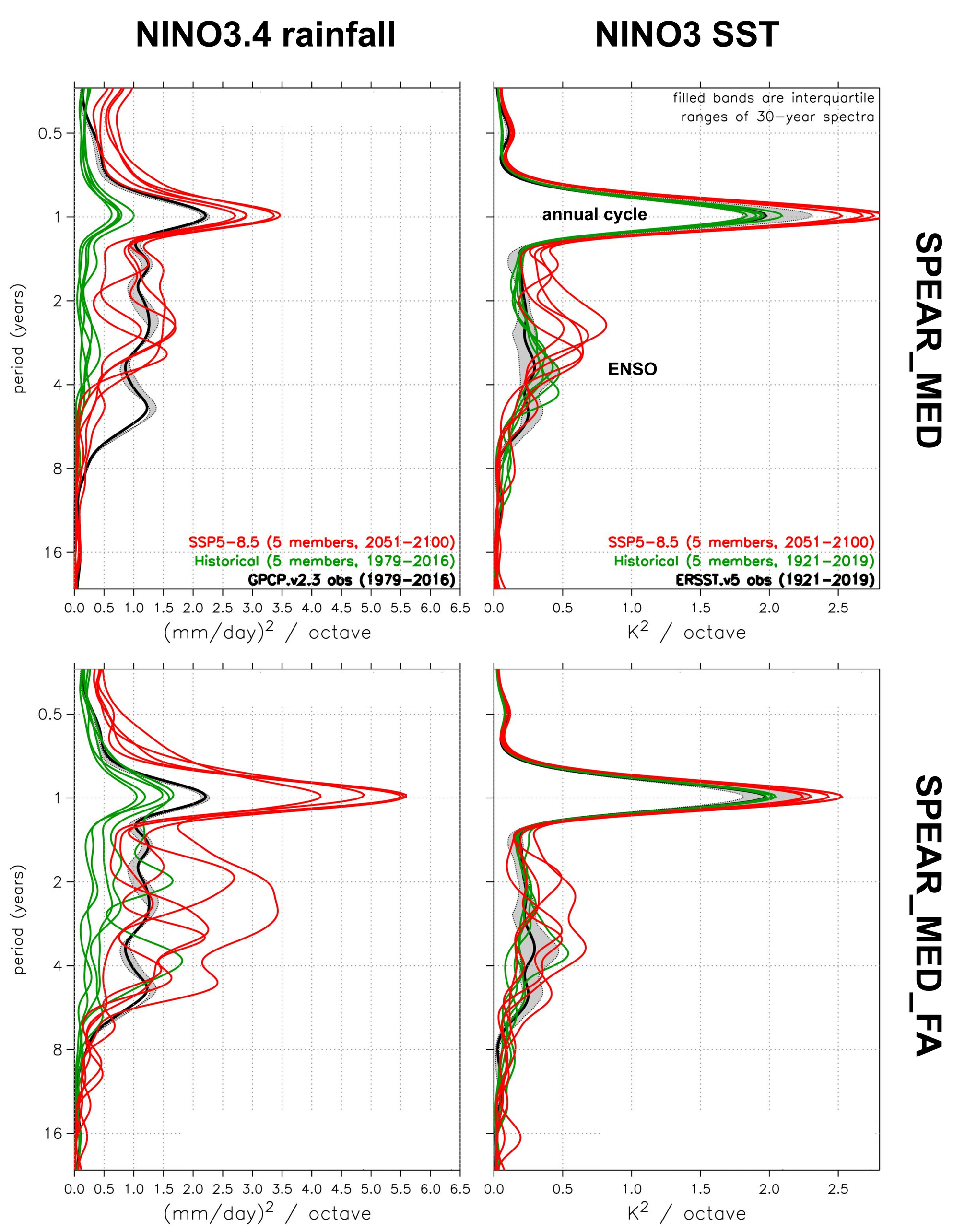

Fig. 7: Time-mean **spectral power** (abscissa) as a function of period (ordinate, in octaves of the annual cycle) from a Morlet wavenumber-6 wavelet analysis. The area to the left of each curve represents the spectral power within a given frequency band. **Black** curve is the observed spectrum for **NINO3.4 rainfall** (left column; mm^2 day^{-2} octave^{-1}, for 1979–2016 from GPCP.v2.3) and **NINO3 SST** (right column; K^2 octave^{-1}, for 1921–2019 from ERSST.v5). **Green** curves are corresponding spectra from the 5 historical ensemble members of SPEAR_MED (top row) and SPEAR_MED_FA (bottom row). **Red** curves are the models' projected spectra for 2051–2100.

That simulations & projections of ENSO are sensitive to the emergent background biases of models, warrants caution when interpreting model-based ENSO outlooks (Ding et al. 2020; Stevenson et al. 2021). Efforts are underway at GFDL and in the broader community to diagnose, understand, and address these model biases and their impacts (e.g. Wittenberg et al. 2018; Ray et al. 2018; Guilyardi et al. 2020; Planton et al. 2021; Lee et al. 2021; Chen et al. 2021). Models with finer atmospheric & oceanic resolution (lateral & vertical), and improved oceanic mixing and atmospheric convection & cloud parameterizations in the tropics, will be crucial for more reliable ENSO outlooks. Such efforts can be nurtured through expanded computing resources and an enhanced Tropical Pacific Observing System (TPOS, (Kessler et al. 2021).

***Dr. Andrew T. Wittenberg, US DOC/GFDL, 201 Forrestal Road, Princeton, NJ 08540-6649. Email: Andrew.Wittenberg@noaa.gov Web: http://www.gfdl.noaa.gov/~atw**